JOURNAL OF GEOPHYSICAL RESEARCH, VOL. 113, C09010, doi:10.1029/2007JC004699, 2008

Click Here for Full Article

Effects of western boundary current dynamics on the internal wave field of the Southeast Florida shelf

Kristen A. Davis,[1] James J. Leichter,[2] James L. Hench,[1] and Stephen G. Monismith[1]

Received 16 December 2007; revised 17 June 2008; accepted 19 June 2008; published 4 September 2008.

[1] Shelf sea internal wave fields are typically highly variable and dominated by wind and tidal forces. However this is not necessarily true for outer shelf regions or very narrow shelves where remote physical processes originating over the slope or deep ocean may exert a strong influence on the internal wave climate. During the summers of 2003 and 2004, observational studies were conducted to examine the effects of a western boundary current (the Florida Current), tides, and wind on the mean currents and internal wave field on the outer Southeast Florida shelf. Wavelet analyses of nonstationary shelf currents coupled with altimetry images of the Straits of Florida reveal the strong influence of Florida Current fluctuations on outer shelf flows. Local winds were found to be a small factor in flows on the outer shelf region and tidal forcing (diurnal and semidiurnal) accounted for less than a third of the total barotropic variance. High-frequency internal waves dominate the internal wave field and result in bottom-intensified currents and strong shoreward mass transport. We present evidence that suggests that the Florida Current plays as large a role in the determination of the high-frequency internal wave field as tidal forces. These observations and analyses show that it is necessary to include the forcing from the Florida Current meanders and instabilities in order to predict accurately the episodic nature of the internal wave field on the Southeast Florida shelf.

Citation: Davis, K. A., J. J. Leichter, J. L. Hench, and S. G. Monismith (2008), Effects of western boundary current dynamics on the internal wave field of the Southeast Florida shelf, *J. Geophys. Res.*, *113*, C09010, doi:10.1029/2007JC004699.

1. Introduction

[2] Internal waves, generated by remote forcing events, propagate onto the continental slope until geometric constraints cause the waves to either reflect back into the ocean interior or to propagate upslope. As the waves shoal they are transformed by the competing effects of nonlinear steepening and dispersive spreading and can form nonlinear internal waves. Internal wave energy on the continental shelf increases turbulence and mixing in the bottom boundary layer and thermocline region [e.g., *Sanford and Grant*, 1987; *Inall et al.*, 2000; *Ivey et al.*, 2000], drives diapycnal mixing [*Sharples et al.*, 2001; *Hosegood et al.*, 2004; *Ledwell et al.*, 2004; *Hales et al.*, 2005], and the shoreward transport of heat, nutrients, sediment, and planktonic larvae [*Pineda*, 1991] through the formation of trapped cores of recirculating fluid [*Klymak and Moum*, 2003; *Lamb*, 2003; *Scotti and Pineda*, 2004].

[3] On many continental shelves, the internal wave field is highly variable and is dominated by wind and tidal forces [*Munk and Wunsch*, 1998]. However on narrow continental shelves or in the outer shelf region, the internal wave field may also be intimately connected to other oceanographic processes such as shelfbreak frontal jets and mesoscale eddies [*Liu et al.*, 1998; *Colosi et al.*, 2001]. These processes can affect stratification on the shelf and can alter the vertical and horizontal shear environment through which internal waves propagate [*Kunze*, 1985; *Baines*, 1986].

[4] This work examines the effects of a western boundary current, tidal forcing, and wind on the internal wave field of the outer Southeast Florida shelf. Field observations were made in the summers of 2003 and 2004 on Conch Reef, a bank-barrier reef at the northern end of the Florida Keys Reef Tract (Figure 1). The proximity of this reef system to the shelf edge and the axis of the Florida Current (FC) results in a dynamic flow environment with an energetic internal wave field particularly in the spring and summer months (March–October) [*Leichter et al.*, 1996].

[5] In an observational study carried out on the Florida Keys Reef Tract, *Leichter et al.* [1996] documented the presence of internal bores traveling up the reef slope at speeds of 0.1 to 0.3 m s^{-1}, characterized by the strong onshore transport of cool, nutrient-rich water near the bed. Further observations [*Leichter et al.*, 2003, 2005] revealed a highly episodic internal wave field with wave forms ranging from regularly spaced, cool-water intrusions correlated with the tide – possibly the leading edge of the internal tide – to more irregular packets of high-frequency waves associated with upslope-surging masses of dense fluid. Observations made by these studies as well as this study indicate a broad continuum of variation in the characteristics of the waves

[1] Environmental Fluid Mechanics Laboratory, Stanford University, Stanford, California, USA.
[2] Scripps Institution of Oceanography, University of California, San Diego, La Jolla, California, USA.

Copyright 2008 by the American Geophysical Union.
0148-0227/08/2007JC004699$09.00

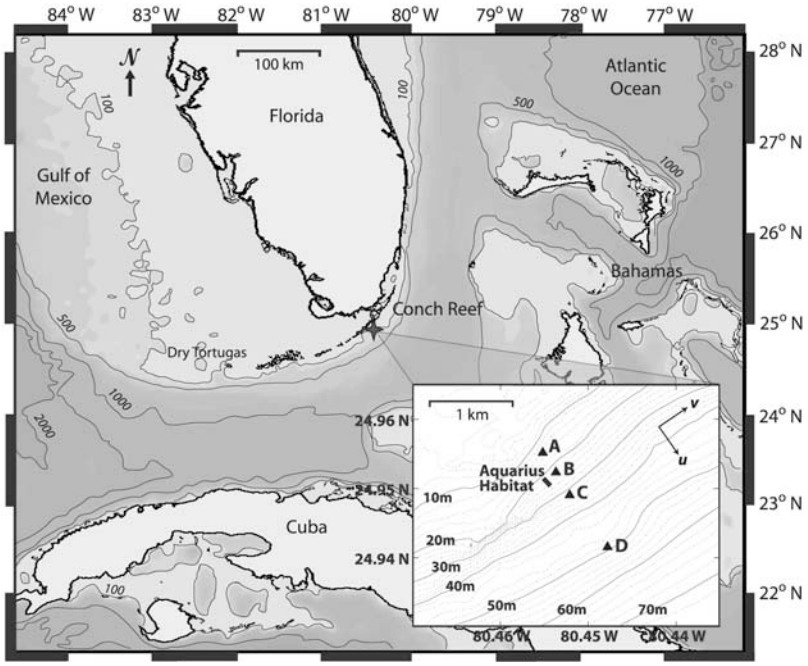

Figure 1. Map of the Straits of Florida region, indicating the location of Conch Reef on the Southeast Florida shelf. Contours are in meters. Inset map is an enlargement of the study site with contoured bathymetry and the location of moorings. Contours on the inset map are in 10-m intervals.

present on the Southeast Florida shelf, especially in the high-frequency band. The high-frequency events can appear as bolus-like, discrete vortices of dense fluid propagating near the bed or as bore-like fronts, and sometimes, seem to have both wave-like and bore-like properties associated with ''solibores'' [*Henyey and Hoering*, 1997]. While variable in form, the high-frequency waves at this site are consistently associated with strong mass transport which indicates nonlinearity in the wave form and for simplification, we refer to these more generally as high-frequency nonlinear internal waves (NLIWs).

[6] The episodic nature of the internal waves on the Southeast Florida shelf indicates that the internal wave field may be modulated by forces in addition to the tide such as changes in shear and stratification driven by the FC [*Leichter et al.*, 2003]. Variations in FC volume transport have been linked to the geostrophic adjustment of stratification in the Straits of Florida [*Stommel*, 1958]. In a thermal-wind balance, an increase in FC transport and thus downstream baroclinic flow would result in increased stratification on the western side of the Straits and could allow internal waves to propagate along the uplifted pycnocline into shallower waters. The passage of cyclonic FC frontal eddies can also cause an uplift of the pycnocline and has been associated with enhanced internal wave activity on the Florida Keys Reef Tract [*Sponaugle et al.*, 2005].

[7] Previous work on the Southeast Florida shelf is clearly suggestive of a link between FC dynamics and the internal wave field. This study utilizes nonstationary spectral methods to understand how broadscale current variability in the FC is related to the internal wave climate on the shelf. It is important to understand the intermittency of internal waves on the Florida Keys Reef Tract because they have the potential to significantly modify the intensity and distribution of turbulent mixing on the shelf and thus to influence mass transfer to benthic organisms. Additionally, the upwelling of cool water by NLIWs may play an important role in the survival and management of coral reef ecosystems plagued by bleaching due to elevated sea surface temperatures [*Riegl and Piller*, 2003].

2. Field Site Description

[8] Conch Reef (24°57.0′N, 80°27.3′W, Figure 1) is located within the Florida Keys National Marine Sanctuary on the Southeast Florida shelf. A bathymetric cross-section of the outer continental shelf and slope at Conch Reef is shown in Figure 2a. In contrast to the broad shelves of the Middle and South Atlantic Bights, the Southeast Florida shelf is narrow (approximately 8 km in width near Conch Reef) and the shelfbreak is shallow (10–20 m depth). The inner and middle shelves are fairly flat (depths ranging 2–10 m) and dominated by sand and seagrass beds with scattered patch reefs. On the outer shelf, bottom topography is more irregular as the density of patch reefs increases toward the reef crest [*Ginsburg et al.*, 2001]. There are two areas on the slope offshore of Conch Reef that have an obvious steepening of the gradient and which could be thought of as the ''shelfbreak'', one at 10–20 m depth and one at 300m depth (not shown in Figure 2a). We define the shelfbreak in this work to be the shallower break in slope just seaward of the reef crest to be consistent with previous literature [e.g., *Lee*, 1986] and because there is a distinct shift in flow regime that is characteristic of shelfbreaks [*Haus et al.*, 2000].

[9] Seaward of the reef crest, the bed slopes steeply from 10 to 30 m and bottom topography is dominated by buttress

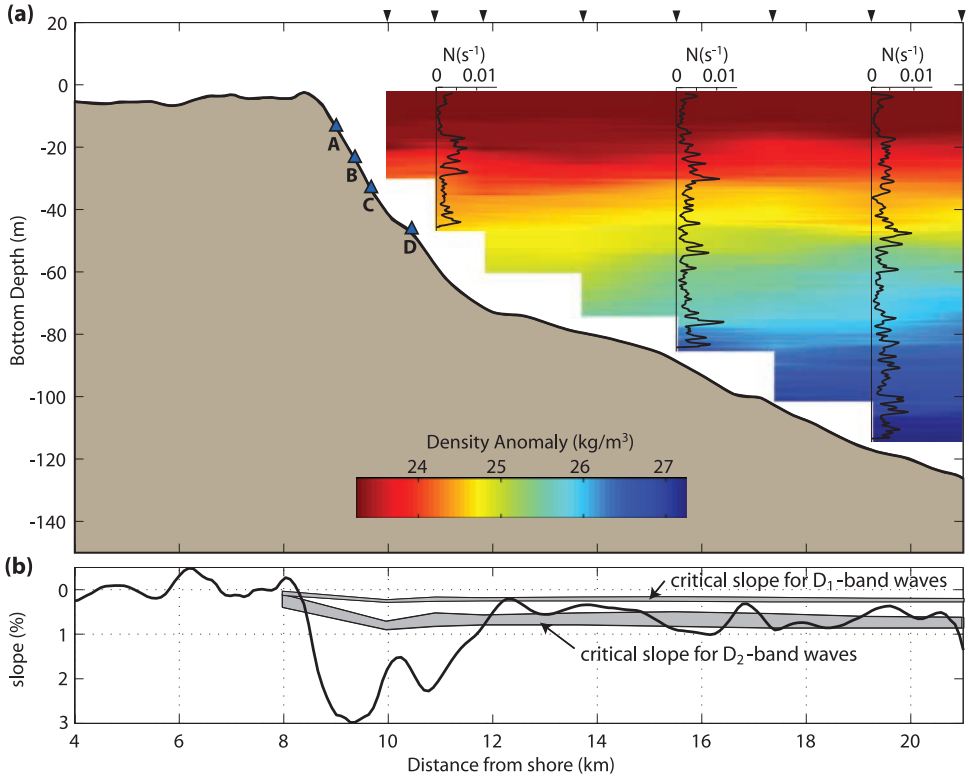

Figure 2. (a) Cross-section of bathymetry on the outer continental shelf and upper slope near Conch Reef. Color contours are density (σ_t) calculated from eight vertical CTD profiles taken on 18 June 2004. Individual casts are marked by black triangles. Profiles of buoyancy frequency, $N(s^{-1})$, are plotted for three casts and were smoothed over 0.5 m in the vertical. Mooring locations are indicated by blue triangles. (b) Average slope of the bathymetry (thick black line) and the ranges of slopes that are near critical for an internal wave of diurnal or semidiurnal frequency (gray patches). Bathymetric data were obtained from the National Geophysical Data Center Coastal Relief model series and averaged over 0.5 km in the alongshelf direction.

and spur-and-groove formations (1 to 2 m in height) separated by sand patches [*Jaap*, 1984]. Bed slope is quite variable on the forereef. An alongshelf average gives a slope of 3%, but in places the forereef can reach 10% to 15% (Figure 2b). Below the 70-m isobath, the bottom slopes more gradually in a sand plain that extends to 300 m depth approximately 35 km offshore. The benthic community shifts from isolated reef patches at 30–35 m depth to sand and macroalgal communities below 40 m [*Leichter et al.*, 2008].

[10] The axis of the Florida Current, with core velocities up to and sometimes exceeding 2.0 m s^{-1} to the northeast, typically lies 5–10 km offshore of the shelf and, as shown below, strongly influences currents on Conch Reef. While FC volume transport through the Straits of Florida is remarkably steady on the timescale of years (averaging approximately 30 Sv), it exhibits large variability on a range of scales from seasonal to tidal [*Brooks*, 1979; *Schott et al.*, 1988]. The annual cycle of FC transport, with a maximum in spring and summer and a sudden decrease (~3–4 Sv) in fall, is thought to be linked to seasonal changes in along-channel winds in the Straits of Florida [*Lee and Williams*, 1988] and remote wind forcing in the North Atlantic [*Schott et al.*, 1988].

[11] Baroclinic instabilities (where potential energy is converted to kinetic energy) in the FC, originating from remote wind forcing or continental shelf waves, can produce FC meanders and frontal eddies resulting in short timescale (days to weeks) variability comparable to that of the annual cycle [*Schott and Duing*, 1976; *Boudra et al.*, 1988; *Lee and Williams*, 1988]. The largest of the cyclonic, cold-core eddies, typically 100–200 km in diameter, are formed near the Dry Tortugas (see Figure 1) and propagate downstream (to the northeast) along the western edge of the FC [*Lee et al.*, 1995]. As the topography of the Straits of Florida converges in the Middle and Upper Keys, the eddies elongate and eventually shear into smaller and faster moving mesoscale (diameter <100 km) and sub-mesoscale (diameter ~10–40 km) eddies [*Haus et al.*, 2000]. Sub-mesoscale frontal eddies can be generated anywhere along the current boundary when the FC meanders offshore and are sometimes followed by a warm, southward-oriented extrusion of FC water onto the shelf [*Lee and Mayer*, 1977; *Lee et al.*, 1981]. These eddies are one of the primary mechanisms of water mass exchange between the FC and the shelf [*Haus et al.*, 2004].

[12] Barotropic (surface) tidal currents in the Straits of Florida are mixed-semidiurnal and relatively small in amplitude (3–5 cm s^{-1}) [*Kielmann and Duing*, 1974]. The interaction of the barotropic tidal currents with the topography of the Straits produces an energetic internal tidal field [*Parr*, 1937; *Schmitz and Richardson*, 1968]. Theoretical

Table 1. Mooring Instrumentation and Configuration

Mooring	Depth (m)	Alongshelf direction (°)	Instrumentation	Configuration	Deployment
A	16	50	Teledyne RDI ADCP	1200 kHz; 0.25 m bins; Δt = 1 s; σ_n = ±1.76 cm s^{-1}	11–20 June 2004
B	20	44	Teledyne RDI ADCP	600 kHz; 0.5 m bins; Δt = 1 min; σ_n = ±1.44 cm s^{-1}	11–20 June 2004
			Seabird SBE39 Temperature Sensors	Depths: 4, 6, 8, 10, 12, 14, 16, 18, and 19 m; Δt = 10 s; σ_n = ±0.002°C	11–20 June 2004
C	32	39	Teledyne RDI ADCP	600 kHz; 1 m bins; Δt = 1 min; σ_n = ±0.90 cm s^{-1}	15 May–8 August 2003 and 11–20 June 2004
			Seabird SBE39 Temperature Sensors	Depths: 7, 12, 17, 22, 27, and 31 m; Δt = 10 s; σ_n = ±0.002°C	11–20 June 2004
D	48	35	Teledyne RDI ADCP	600 kHz; 2 m bins; Δt = 1 min; σ_n = ±0.48 cm s^{-1}	15 May–8 August 2003 and 11–20 June 2004

modeling [*Stommel*, 1958; *Niiler*, 1968] suggests that a cross-channel, baroclinic oscillation can be excited by a long barotropic wave traveling along a non-uniform channel. If the period of the surface wave is close to the natural period of the internal seiche (10–12 hours for the Straits of Florida), the baroclinic oscillation can become large. This is true for the semidiurnal surface tide which travels south through the Straits of Florida. *Soloviev et al.* [2003] refer to this cross-channel seiche mechanism as a possible explanation for 10-hour period internal oscillations observed on the shelf off of Port Everglades, Florida (approximately 125 km northeast of the study site).

3. Methods

[13] The study on Conch Reef was carried out in two phases. During the first phase, from May to August 2003, an 85-day record of currents and bottom temperature was collected on the slope offshore of the reef at Moorings C and D (Figure 1) using RD Instruments Workhorse 600 kHz Acoustic Doppler Current Profilers (ADCPs). Profiles of conductivity and temperature were measured seaward of the reef during a cruise on the R/V Waltonsmith on 15 September 2003 using a Seabird Electronics SBE-19 CTD profiler. Eight CTD casts were made at stations spaced along a line (150° heading) running from Conch Reef to a location 18 km offshore (Figure 2a).

[14] During the second phase of the study, in June 2004, a densely instrumented moored array was deployed on Conch Reef to resolve cross-shelf variations in mean flow and internal wave dynamics. Instruments were configured in a cross-shelf profile extending from the 16 m isobath (Mooring A), just seaward of the reef crest, to the 48m isobath, 1 km offshore of the reef crest (Mooring D). Mooring B, at 20 m depth, was located on a reef spur above the steepest part of the slope and Mooring C, at 32 m depth, was positioned at the base of the reef spur-and-groove structure. Velocity measurements at all moorings were collected with upward-looking ADCPs mounted to the bottom and the data from each instrument were rotated into local alongshelf (v), across-shelf (u), and vertical components (w). The rotation angle for each mooring is given in Table 1. Nine days of overlapping data were collected during a period of intense internal wave activity, 11–20 June 2004. Table 1 shows instrument configuration for each mooring and approximate error due to instrument noise as estimated by the manufacturer. All times refer to local time, Eastern Daylight Time (EDT = Greenwich Mean Time (GMT) - 4).

[15] In ADCP measurements, horizontal inhomogeneities in the velocity field of a scale comparable to and smaller than the distance separating the beams can cause errors in the data by the contamination of one velocity component with another [*Scotti et al.*, 2005]. "Error velocity", calculated as the difference between the estimates of vertical velocity from two independent pairs of beams, can help flag data that violates the local homogeneity condition [*Lu and Lueck*, 1999]. For data collected during this study, error velocities were observed to be above instrument noise level in less than 2% of all velocity measurements.

[16] Time series measurements of temperature on the reef slope were obtained using vertical arrays of Seabird Electronics SBE-39 temperature sensors, deployed on taut lines at Mooring B and C. The temperature sensors sampled every 10 seconds and were spaced at 2-m intervals on Mooring B and 5-m intervals on Mooring C (see Table 1 for further details). Additionally, four offshore profiles of temperature and conductivity were collected with a Seabird SBE-19 CTD (on 9, 16, 18, and 22 June) using the same stations as the 2003 study.

4. Data Analyses

[17] Velocity data were averaged into 1-hr blocks and subsequently separated into barotropic and baroclinic components. As an alternative to the standard depth-averaged definition of barotropic velocity, we performed a complex empirical orthogonal function (CEOF) analysis on the horizontal currents (u + iv) at each station [*Stacey et al.*, 2001] and defined the barotropic component to be the current which corresponds first vertical mode and the baroclinic component as the current which corresponds to the summation of the second through fifth vertical modes (which represents the first through fourth baroclinic modes). Because of acoustic reflection from the water surface in the ADCP measurements, velocity was not recorded in the top 13% of the water column. Despite this missing data, the first four baroclinic modes can be adequately resolved and account for greater than 99% of the variance in the baroclinic velocity.

[18] The shape of the barotropic mode (Figure 3a) exhibits a reduction in magnitude near the bed due to frictional effects and is well predicted by a logarithmic boundary

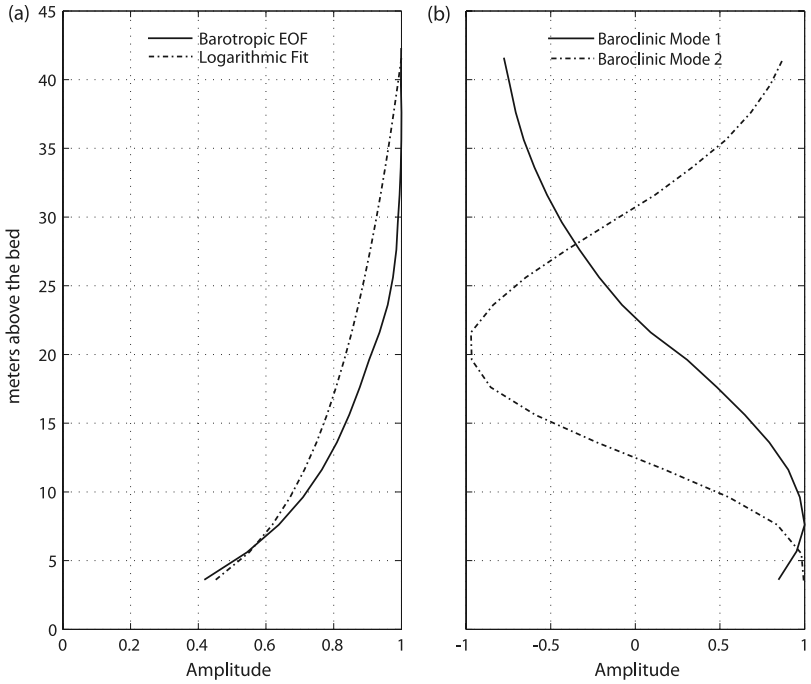

Figure 3. (a) The barotropic mode determined from a CEOF analysis of horizontal currents at Mooring D in the 2003 study (solid line) and a logarithmic fit to the barotropic profile (dotted line), and (b) the first two baroclinic modes predicted by CEOF analysis.

layer profile. The first two baroclinic modes (Figure 3b) show significant structure over the water column, suggesting stratification is important. Here we use v_{bt} and u_{bt} to denote along- and across-shelf barotropic currents and v_{bc} and u_{bc} for along- and across-shelf baroclinic currents.

[19] A dynamical analysis of nonstationary shelfbreak currents requires a method that can represent a signal as a function of both frequency and time. We employed continuous wavelet transforms (CWTs) to examine the spectral content of the data. CWTs are a common tool for analyzing the time-varying frequency content of nonstationary signals in many fields, and have recently been used in oceanographic applications [e.g., *Liu and Miller*, 1996; *Jay and Kukulka*, 2003]. The method is based upon an oscillatory wavelet function (or "mother wavelet"), $\psi_0(\eta)$, where η is a non-dimensional time parameter and the function has zero mean, finite variance, and is localized in time near the origin so that oscillations decay at infinity. A time series signal is transformed into time-frequency space through convolution with a set of scaled and translated versions of the mother wavelet function. We used the Morlet wavelet function, given by

$$\psi(\eta) = \pi^{-1/4} e^{i\omega_0 \eta} e^{-\eta^2/2} \tag{1}$$

which is a plane wave modulated by a unit width Gaussian, where ω_0 is a non-dimensional frequency, taken here to be equal to 6 [*Farge*, 1992]. The complex-valued Morlet wavelet function provides information about both amplitude and phase. Other wavelet bases (such as the "Mexican hat" and "Paul") were tested and gave the same qualitative results. Scales for the CWT were chosen to resolve the major tidal frequencies with sufficient redundancy (20 "voices" per octave) so that the wavelet transform preserves variance and the time series could be accurately reconstructed. The transform was performed in Fourier space following the methods outlined in *Torrence and Compo* [1998]. For the Morlet function, the wavelet scale, s, is almost identical to the Fourier period, and therefore, we will refer to "scale" and "period" interchangeably. The wavelet power spectrum is defined as the magnitude of the wavelet transform, squared, $\mathcal{W} = |\mathcal{W}_n(s)|^2$, where n is a localized time index. "Scale-averaged" wavelet power can be used to examine wavelet power over a range of scales, s_1 to s_2 (index j_1 to j_2),

$$\langle \mathcal{W} \rangle = \frac{\partial j \partial t}{C_\partial} \sum_{j=j_1}^{j_2} \frac{|\mathcal{W}_n(s)|^2}{s_j} \tag{2}$$

where ∂j is a factor determining scale resolution, ∂t is the time series interval, and C_∂ is a reconstruction constant [*Torrence and Compo*, 1998].

[20] Tidal ellipses are a useful way to show how tidal currents vary in space. Ellipse parameters are typically determined from harmonic constants obtained by doing a harmonic analysis on the measured current vectors. However harmonic analysis assumes a relatively stationary current field and, when performed on the nonstationary currents measured during the 2003 and 2004 studies, did not accurately capture the tidal dynamics. As an alternative to the traditional tidal current ellipses, we constructed tidal variance ellipses, where ellipse parameters were determined using the method of principal variances [*Preisendorfer*, 1988]. Velocity measurements are band-passed to isolate currents of tidal frequencies (diurnal band, 20–34 hours and semidiurnal band, 11–14 hours) and the residual velocities

in each band are found by subtracting the time average. The principle variances of the velocity measurements are

$$\left.\begin{matrix}\lambda_1\\ \lambda_2\end{matrix}\right\} = \frac{1}{2}\left\{\left(\overline{u'^2}+\overline{v'^2}\right) \pm \left[\left(\overline{u'^2}-\overline{v'^2}\right)^2+4\left(\overline{u'v'}\right)^2\right]^{1/2}\right\} \quad (3)$$

where u' and v' are the across-shelf and alongshelf velocity fluctuations obtained by removing the respective means $\overline{u}$ and $\overline{v}$ from each record, λ_1 gives the variance of flow along the major axis of the ellipse, and λ_2 gives the variance along the minor axis. The orientation of the major axis is given by the principal angle

$$\theta_p = \frac{1}{2}\tan^{-1}\left[\frac{2\overline{u'v'}}{\overline{u'^2}-\overline{v'^2}}\right] \quad (4)$$

which is defined in the range $-\pi/2 \le \theta_p \le \pi/2$.

5. Observations

5.1. Stratification

[21] The average stratification observed during both 2003 and 2004 studies was typical for summer conditions on the Southeast Florida shelf and upper slope [*Leichter et al.*, 1998, 2003, 2007]. A cross-shelf profile of density, ρ, and buoyancy frequency, $N=\left(-\frac{g}{\rho_0}\frac{\partial\rho}{\partial z}\right)^{1/2}$ (where g is acceleration due to gravity and ρ_0 is a reference density), from a CTD transect performed near the end of the 2004 experiment is shown in Figure 2a. Data from this transect are representative of offshore conditions observed during both studies. Summer stratification just offshore of the shelfbreak can be generally characterized as a relatively well-mixed upper layer that ranges in thickness from 10–50 m and a lower layer with step-like density profile extending to the bed. A persistent feature in most CTD casts is a region of elevated stratification near the bed. Typical buoyancy periods were 10 minutes in the surface layer and 5–6 minutes in the lower layer with peaks in stratification of 1–2 minute periods scattered throughout the lower layer and commonly near the bed. Data from the vertical array of temperature sensors at Mooring B indicate that on the shallow shelf N was variable in time, but generally increased with depth. In the range of temperatures found on the reef tract, 22–30°C, density varied primarily with temperature.

[22] The slope of the averaged bathymetry profile at the study site and the ranges of slopes that would be critical for a linear internal wave of diurnal or semidiurnal frequency are shown in Figure 2b. The ranges of critical slopes were identified by the ratio $\alpha/s = 1$, where α is the bathymetric slope and s is the slope of the internal wave characteristic [*Phillips*, 1977]:

$$s = \tan\theta = \left(\frac{\omega^2-f^2}{N^2-\omega^2}\right)^{1/2} \quad (5)$$

θ is the angle of the internal wave characteristic, ω is the internal wave frequency, f is the Coriolis frequency which is 6.15×10^{-5} rad s^{-1} at 25°N, and N is a range of near-bed buoyancy frequencies recorded throughout the study. For semidiurnal period internal waves, the slope of the bed offshore of Conch Reef (Figure 2b) is supercritical ($\alpha > s$) from the shelfbreak to the 70-m isobath (4 km from the shelfbreak) and approximately critical from the 70-m isobath to the 125-m isobath, (13 km from the shelfbreak). For diurnal period internal waves, the slope of the bed seaward of the shelfbreak is almost entirely supercritical. CTD profiles were not taken past the 125-m isobath and the criticality of the slope beyond this station could not be calculated.

5.2. Barotropic Currents

[23] To investigate the effect of large scale oceanographic dynamics on outer shelf circulation we examined an 85-day current record taken at the seaward-most station (Mooring D) from May to August 2003. Time series of barotropic alongshelf (v_{bt}) and across-shelf (u_{bt}) velocities (Figures 4a and 4d) were decomposed into frequency-time space using CWTs (described in section 3) resulting in contours of wavelet power (Figures 4b and 4e). To test the significance of the wavelet power spectrum, peaks were compared to a background model spectrum of red-noise [*Qiu and Er*, 1995; *Torrence and Compo*, 1998]. Wavelet power peaks above the background spectrum are assumed to be significant features. In a plot of wavelet power, stationary processes produce horizontal contours, while nonstationary "events" form vertical contours.

[24] Both the time series and wavelet representations of the 2003 data set exhibit a large degree of unsteadiness with the most striking feature being a dramatic shift in current regime between early summer (15 May–30 June) and late summer (1 July–8 August). In early summer barotropic currents are primarily to the northeast, in the same direction as the FC, with an average speed of 13 cm s^{-1}. In July and early August 2003 the average barotropic current speed rose to 30 cm s^{-1} and velocity variance was more than twice that of early summer. Large amplitude current oscillations persisted throughout the month of July, punctuated by week-long periods of strong downcoast flow (to the southwest). These events appear as vertical contours in wavelet power with peaks broadly distributed across the spectrum (Figures 4b and 4e).

[25] Time-averaged wavelet power, $\langle\mathcal{W}\rangle$ (Figures 4c and 4f), and scale-averaged wavelet power, $\overline{\mathcal{W}}$ (Figure 4g), were calculated for both along- and across-shelf components of the barotropic velocities. Time averages were performed separately for early and late summer to highlight the difference in spectral power between these periods. Both averaging schemes reveal a considerable enhancement of spectral energy across all periods in late summer, but in the time-averaged representations, the increase in energy is especially pronounced in the inertial-diurnal band.

[26] Eddy-like instabilities were identified in the record (gray shading in Figures 4 and 4d) by comparing the observed currents with the pattern characteristic of a moving vortex [*Lee*, 1975, see further discussion below]. A series of three eddy-like oscillations, most obvious in the time series of u_{bt} (Figure 4d) passed through the domain during 6–8 June, accompanied by a broad peak in wavelet power in the inertial-diurnal band in v_{bt}, and a peak spanning periods from 3 hours to diurnal in u_{bt}. This spectral cascade suggests that energy input through low-frequency processes in the alongshelf direction is transferred to energy in higher-

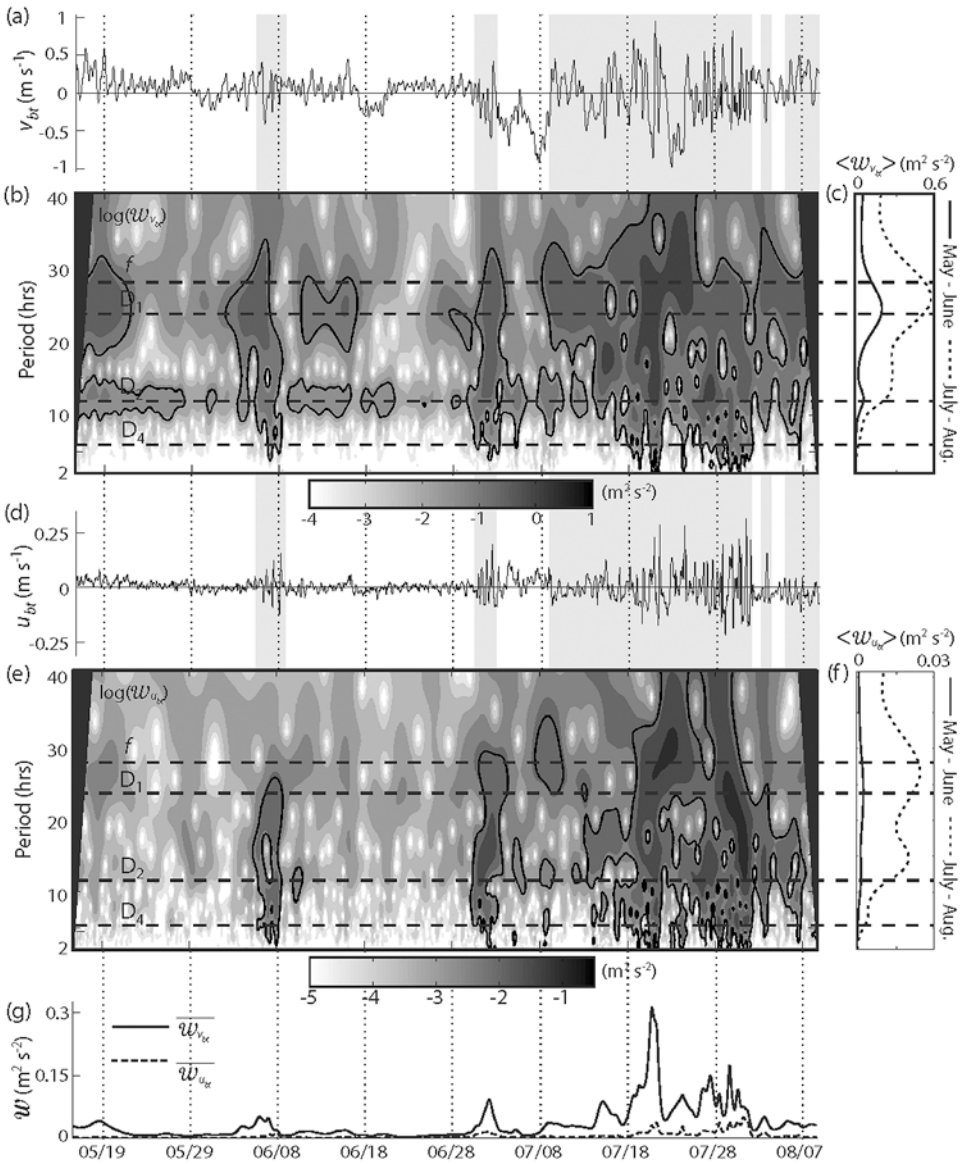

Figure 4. Barotropic currents measured at Mooring D, summer 2003. (a) 1-hr averaged alongshelf velocity, v_{bt}, (b) logarithm of the wavelet power spectrum for v_{bt}, $\mathcal{W}_{v_{bt}} = |\mathcal{W}_{v_{bt}}(s)|^2$, (c) time-averaged wavelet power for v_{bt}, $\langle \mathcal{W}^{v_{bt}} \rangle$; averages are taken over the first half of the summer (15 May-30 June) and the second half of the summer (1 July–8 August), (d) 1-h averaged across-shelf velocity, u_{bt}, (e) logarithm of the wavelet power spectrum for u_{bt}, $\mathcal{W}_{u_{bt}} = |\mathcal{W}_{u_{bt}}(s)|^2$, (f) time-averaged wavelet power for u_{bt}, $\langle \mathcal{W}^{u_{bt}} \rangle$, (g) scale-averaged wavelet power for both components. In panels (b) and (e) the thick black lines are 95% confidence level and dashed horizontal lines mark the major tidal (D_1 is diurnal and D_2 is semidiurnal) and local inertial (f) periods. Darkly shaded regions on either side of the wavelet spectra indicate the "cone of influence" where edge effects become important.

frequency processes in the across-shelf direction, providing insight into the flow of energy during an eddy-like instability, one of the primary mechanisms for water mass exchange over the shelfbreak.

[27] Because of the limited spatial extent of this data set, it is difficult to determine with complete certainty whether the oscillatory instabilities observed are produced by frontal eddies or near-inertial propagating waves, as these processes have similar characteristic time and length scales. Frontal eddies in the Upper Florida Keys have been observed to range from 10–30 km in diameter and are advected upcoast by the FC at 20–80 cm s^{-1} [*Lee and Mayer*, 1977; *Haus et al.*, 2000] and near-inertial waves previously observed in the lower Keys have wavelengths of approximately 40 km and propagate upcoast at 30 cm s^{-1} [*Shay et al.*, 1998].

[28] The current and temperature patterns observed for the eddy-like oscillations in the 2003 study were compared to a kinematic model of FC "spin-off" eddies developed by *Lee* [1975], which superimposes a moving vortex pair on a uniform background flow to simulate the currents that

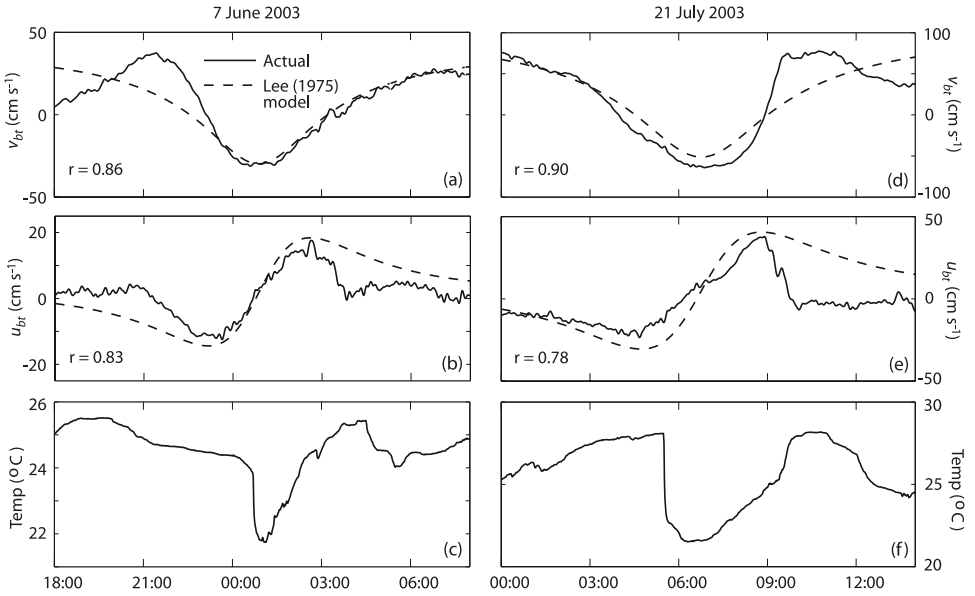

Figure 5. Eddy events recorded at Mooring D on 7 June and 21 July 2003. (a) and (d) show actual alongshelf barotropic currents and modeled alongshelf currents using formulation in *Lee* [1975], (b) and (e) show actual and modeled across-shelf barotropic currents, and (c) and (f) show actual bottom temperature. Correlations between model and observations are noted in each part. Note different vertical scales for each event.

would be seen by a fixed current meter. Figure 5 illustrates the comparison for two events, the first on 7 June and the second, 21 July. In both cases the model generally agrees well with the observed currents, predicting the signature pattern of a strong cyclonic current reversal. Measurements reveal a less symmetric vortex with alongshelf velocities slightly larger and across-shelf velocities somewhat smaller in magnitude than model predictions. While heat advection was not included in the model, observations show an abrupt drop in temperature occurring approximately mid-way through the passage of the instability (Figures 5c and 5f), typical of a cold-core cyclonic eddy. According to model predictions, the 7 June event was estimated to have an 18-hour period and 32 cm s^{-1} phase speed, and the 21 July event, a 24-hour period and 27 cm s^{-1} phase speed. Although *Lee's* [1975] kinematic eddy model is useful for identifying the characteristic currents associated with an individual eddy event, it does not neatly apply to all of the oscillatory events observed, some of which are likely the superposition of multiple instabilities shed from the FC.

[29] Barotropic velocity variances were calculated through spectral methods for data from all moorings during 2003 and 2004 studies (Table 2). Variance in several frequency bands (low-frequency band, >34 hours; diurnal band, 20–34 hours; semidiurnal band, 11–14 hours; high-frequency band, <5 hours) are given as percentages of the total variance. Total variance in alongshelf barotropic velocity, $\sigma_{v_{bt}}^2$ was an order of magnitude larger than the across-shelf direction at all moorings and increases with distance offshore (from Mooring A to D). High-frequency processes account for more than 30% of the total variance in u_{bt} with the exception of Mooring D during the 2003 study, while low-frequency band variance dominates v_{bt}. Variances in the semidiurnal and inertial-diurnal bands together account for 23–32% of the total variance in the barotropic currents.

[30] Tidal variance ellipses (described in section 4) were constructed from tidal band barotropic velocity components from the 2004 study (Figure 6). 95% confidence intervals were calculated for the barotropic ellipse parameters using bootstrapping methods [*Efron and Tibshirani*, 1993] and were found to be ±0.02 cm s^{-1} for both the major and minor axes amplitudes and ±0.3° for the ellipse orientation angle. The major axes of the ellipses are oriented approximately parallel to local isobaths and ellipticity (ε, the ratio of the major to minor axis amplitude) decreases toward shore, reflecting a relatively stronger across-shelf tidal current near

Table 2. Barotropic Velocity Variances for the 2003 (in Parentheses) and 2004 Studies

	u_{bt}, Across-shelf Velocity				v_{bt}, Alongshelf Velocity			
Mooring	A	B	C	D	A	B	C	D
Total variance (cm^2 s^{-2} × 10^{-4})	8.5	7.1	3.1 (7.4)	2.3 (25)	100	130	150 (380)	230 (650)
Variance in frequency bands as a percentage of total variance								
Low-frequency band (>34 hours)	16%	22%	17% (13%)	8% (15%)	44%	42%	42% (46%)	52% (53%)
Inertial-diurnal band (20–34 hours)	8%	6%	6% (14%)	14% (17%)	18%	17%	19% (19%)	20% (17%)
Semi-diurnal band (11–14 hours)	8%	6%	4% (7%)	7% (10%)	12%	14%	13% (7%)	8% (6%)
High-frequency band (<5 hours)	31%	42%	48% (35%)	46% (17%)	4%	4%	2% (2%)	1% (2%)

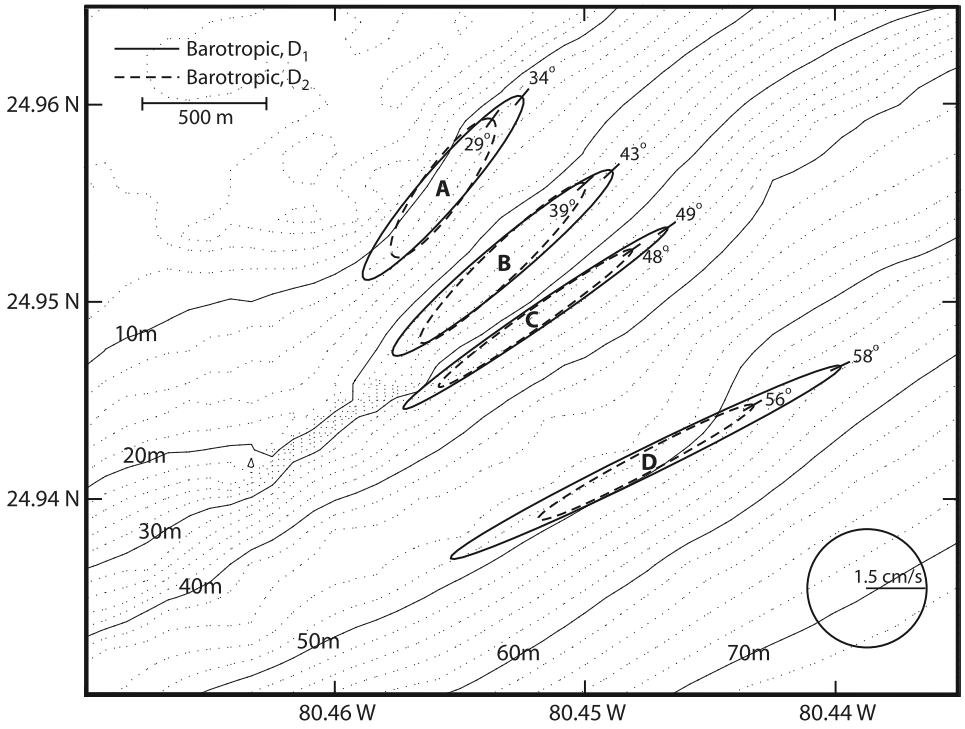

Figure 6. Barotropic tidal ellipses for diurnal (D_1) and semidiurnal (D_2) constituents. Major axis direction relative to true north is indicated for each ellipse.

the shelfbreak. The amplitudes of the barotropic D_1 (diurnal) and D_2 (semidiurnal) ellipses at Mooring D are 5 cm s^{-1} and 3 cm s^{-1}, respectively, and agree with tidal currents observed in the Straits of Florida [*Kielmann and Duing*, 1974].

[31] Local wind data for summer 2003 and 2004 (from the National Buoy Data Center C-MAN station #MLRF1 on Molasses Reef, 10 km to the northeast of the study site), show that winds during both studies were primarily out of the southeast (directed nearly onshore) with speeds generally less than 5 m s^{-1}. 1-hour-averaged wind data did not exhibit a significant correlation with the barotropic velocities during either year. This result is consistent with previous studies in the Upper Florida Keys which have found local wind forcing to be a small factor in flows on the outer shelf region during summer [*Lee and Mayer*, 1977; *Lee*, 1986].

5.3. Baroclinic Currents

[32] While the barotropic mode dominates alongshelf velocities near the shelfbreak, comprising approximately 90% of the variance in *v*, baroclinic modes play a larger role in the across-shelf dynamics, accounting for just over half of the variance in *u* in the 2003 study and up to 90% during periods of elevated internal wave activity. To examine the distribution of energy within the across-shelf baroclinic component, vertical profiles of variance, $\sigma_{u_{bc}}{}^2$, were calculated in the diurnal, (20–34 hours), semidiurnal, (11–14 hours), and high-frequency (<5 hours) bands using spectral methods (Figure 7). Tidal bands (D_1 and D_2) account for close to 20% of the variance in across-shelf baroclinic velocities at Mooring D, but <10% at the shallower moorings. The semidiurnal band u_{bc} is most energetic at Mooring D and exhibits a near-bed variance maximum that is not seen at the shallower moorings. At all moorings, semidiurnal band $\sigma_{u_{bc}}{}^2$ has a maximum near the surface and bottom and a minimum in the middle of the water column. At Moorings C and D, data from the 2003 and 2004 studies exhibit comparable variances. While the observed vertical structure appears similar to that of a mode-one internal wave, modal solutions are not valid for near-critical slopes [*Wunsch*, 1969]. However while the bathymetric slope off Conch Reef is near critical for tidal band waves, it is not critical for higher-frequency waves defined by,

$$\omega > \sqrt{\frac{f^2 - \alpha^2 N^2}{1 + \alpha^2}} \tag{6}$$

obtained by rearranging equation (5). Using an average *N* of 144 cycles per day (cpd) and the maximum bed slope in the shelfbreak region of 0.03, the lowest frequency wave whose characteristic slope is everywhere greater than the bathymetric slope is 4.8 cpd. This restriction was used to define the lower bound of the high-frequency band used in the variance analyses.

[33] Tidal variance ellipses (described in section 4) and confidence intervals were calculated for 2004 semidiurnal baroclinic currents at Moorings B, C, and D at the top, middle, and bottom of the water column (Figure 8). Tidal band u_{bc} recorded at Mooring A approached instrument noise levels and was not included in the analysis. 95% confidence intervals were found to be ±0.02 cm s^{-1} for both the major and minor axes amplitudes and ±5° for the ellipse orientation angle.

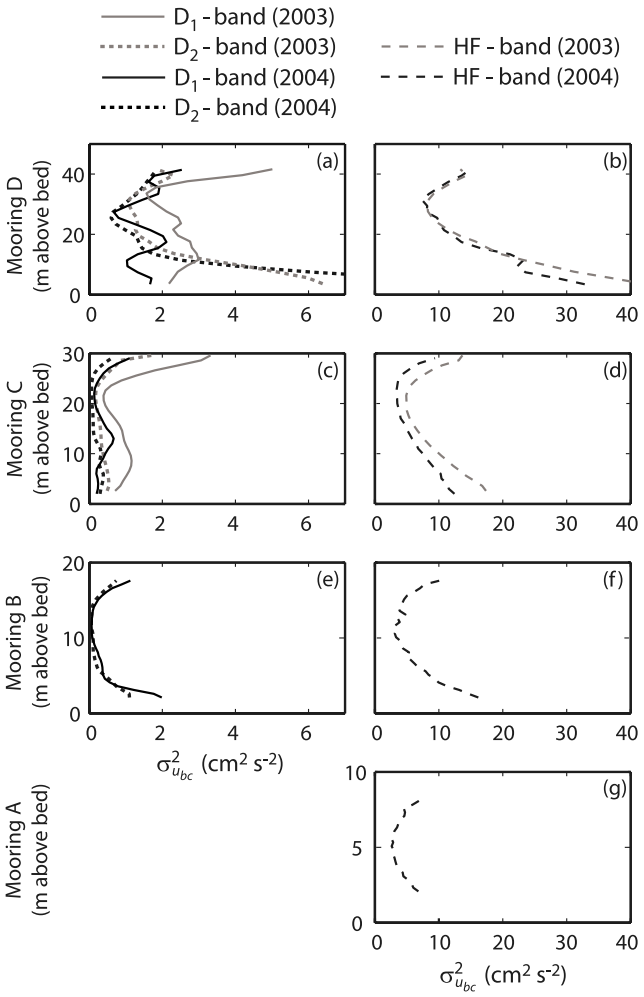

Figure 7. Across-shelf, band-averaged, baroclinic velocity variances as a function of depth at all moorings during 2003 and 2004 studies. D_1 and D_2 band variance is shown in panels (a), (c), and (e). High frequency variance is shown in panels (b), (d), (f), and (g). Tidal band u_{bc} recorded at Mooring A approached instrument noise levels, and was not included in the variance analysis.

[34] For a freely propagating, linear internal wave, the major axis of the baroclinic current ellipse points in the direction of wave propagation and the ellipticity should be approximately $\omega/f = 2.27$ for semidiurnal waves at 25°N [*Gill*, 1982]. Under negligible mean flow conditions, internal waves propagating onto the shelf undergo topographic refraction, turning so that the major axis of the ellipse is approximately perpendicular to the local isobaths [*McKee*, 1973]. The presence of a mean alongshelf flow will tend to rotate the major axis of the ellipse downstream [*Pringle and Brink*, 1999]. Nonlinear internal waves, such as those observed on the outer Southeast Florida shelf, would not be expected to conform to the theoretical shape for a linear internal wave ($\varepsilon \sim \omega/f$) however it is useful as a basis of comparison.

[35] The baroclinic semidiurnal ellipses observed on Conch Reef exhibit a high degree of spatial variability which suggests the presence of finescale structure in the internal wave field on the shelf. The vertical variation in ellipse size is consistent with Figure 7, showing the intensification of semidiurnal band energy at the top and bottom of the water column. The reduction in size of the current ellipses toward shore is an indication that the source of semidiurnal internal wave energy is offshore and is being dissipated as the waves propagate upslope. This agrees with observations of lags between moorings in near-bed current and temperature (see further discussion below) revealing an onshore propagation direction of tidal period waves. With this constraint, the 180° ambiguity in propagation direction can be resolved and it can be said that on average the semidiurnal internal waves propagate upcoast (to the northeast) and onshore. The observed variability in ellipse orientation may be due to the dynamical adjustment of the internal waves to the complex topography of the shallow shelf. Baroclinic ellipses at Moorings B and D at the top and bottom of the water column have a significant cross-shelf component to their orientation and $\varepsilon \sim 2$, while ellipses at Mooring C are more elongated in shape ($\varepsilon \sim 3.5$) and aligned with the bathymetry due to topographic steering from a large spur southwest of the mooring.

[36] Wavelet transforms were performed on the CEOF baroclinic current amplitude in both along and across-shelf components (Figures 9a and 9c). The wavelet power was scale-averaged (equation (2)) over the high-frequency range (Figures 9b and 9d) and represents the energy in the observed high-frequency internal wave field. To visualize the covariance between the high-frequency internal wave field and tidal and sub-tidal processes, scale-averaged diurnal band barotropic current $\overline{\mathcal{W}}$ (representing FC dynamics) and semidiurnal band barotropic current $\overline{\mathcal{W}}$ (representing the surface tide) are also shown. Additionally, shaded patches denoting periods where FC instabilities are passing through the study area are replotted from Figure 4. With this representation, it can be seen that peaks in high-frequency baroclinic wavelet power (thin gray line) roughly correspond to FC instability events on the outer shelf. Correlations between high-frequency, baroclinic $\overline{\mathcal{W}}$ and D_1 and D_2 band barotropic $\overline{\mathcal{W}}$ are of similar magnitude (r = 0.40 within 95% confidence) and significantly different from zero.

6. Discussion

6.1. Influence of Florida Current Dynamics on the Outer Shelf Flow Environment

[37] Typically, currents in shelf-waters are controlled by surface tides and local winds, but on the outer shelf, where the coastal seas meet the deep ocean, internal tides, alongslope currents, and eddies can exert a greater influence. *Lee* [1986] observed this pattern on the Southeast Florida shelf where he found two distinct flow regimes: the inner shelf, where tidal and wind forcing controls current and temperature variability, and the outer shelf, where fluctuations in the FC dominate the flow environment.

[38] Our outer shelf measurements taken during 2003 and 2004 on Conch Reef reinforce this concept. Local winds were found to play a negligible role in barotropic current variability and surface tides (taken as the sum of the diurnal and semidiurnal bands) accounted for less than a third of the total barotropic variance. The summation of the diurnal and

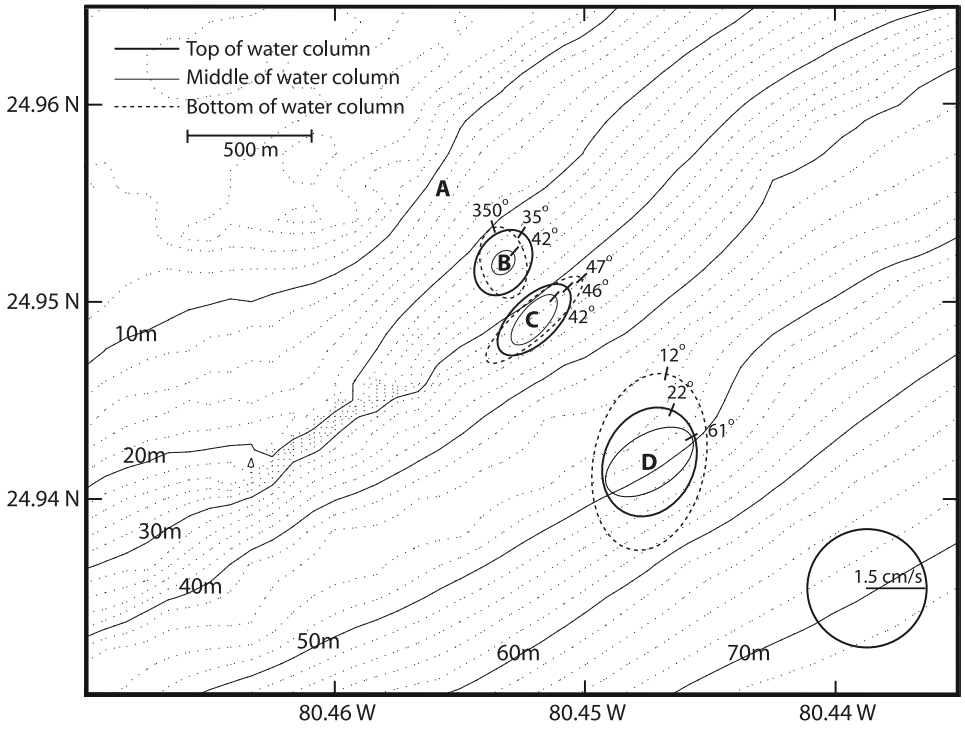

Figure 8. Baroclinic semidiurnal tidal ellipses at the top, middle, and bottom of the water column. Major axis direction relative to true north is indicated for each ellipse.

semidiurnal band variance most likely results in an overestimate of the contribution of surface tides to baroclinic variance since instabilities in the FC also have a near-diurnal spectral signature in the Upper Keys (see Figure 4). Techniques such as harmonic analysis that would typically be used to isolate the diurnal tidal signal from other diurnal band phenomena were not useful with this data set because of the unsteady and episodic nature of the flows.

[39] Wavelet spectral analysis (Figure 4) reveals the strong influence of FC fluctuations on outer shelf flows. Broad, vertical peaks in the inertial-diurnal band reflect the stochastic forcing of mesoscale instabilities in the current structure of the FC such as meanders and frontal eddies [*Lee and Mayer*, 1977; *Brooks*, 1979; *Schott et al.*, 1988]. The dramatic shift in current regime observed in the barotropic velocities between the beginning and end of the summer of 2003 reflects a change in the position of the FC axis offshore of the study site. The cross-channel position of the FC axis as it passes through the Straits of Florida is strongly influenced by the path that it takes before entering the southern Straits as well as by the formation of eddies on the cyclonic front [*Lee et al.*, 1995]. Altimeter data from TOPEX/POSEIDON [*Leben et al.*, 2002] indicate that in late May and early June 2003 the current did not penetrate deep into the Gulf of Mexico (to form the Loop Current), but instead turned east just above the western tip of Cuba and entered the Straits very close to the Dry Tortugas and Lower Keys (Figure 10a). In July 2003 however the Loop Current was reestablished in the Gulf (see Figure 10b) and the current's path took a more southerly course, causing it to overshoot the entrance to the Straits, pushing the axis closer to the coast of Cuba than to the Keys (Figure 10c). The large scale displacement of the FC axis offshore of the lower Florida Keys Reef Tract and convergence of the current with the Southeast Florida shelf in the Middle and Upper Keys could explain some of the frequent and large magnitude instabilities observed in the barotropic velocity record during July and early August at Conch Reef. Energy from FC instabilities permeates the outer shelf and enhances the spectral power across a broad range of time scales, but is especially pronounced in the inertial-diurnal band (see early and late summer $\langle \mathcal{W} \rangle$, Figures 4c and 4f).

6.2. Tidal and Sub-Tidal Influences on the Outer Shelf Internal Wave Field

[40] During the summer, internal waves are a common feature of the circulation on Conch Reef. They play a significant role in outer shelf dynamics, driving strong near-bed flows accompanied by rapid temperature changes that can be as large as the annual range of water temperature on the shelf [*Leichter et al.*, 1996]. A wavelet analysis of CEOF baroclinic current amplitude on the outer shelf, Figure 9, reveals baroclinic energy in a broad spectrum, from f to N, corresponding to a wide range of processes including the regular ebb and flood of the internal tide, the onshore propagation of cool-water internal bores, and high-frequency (near N) internal waves.

[41] While identification of specific generation mechanisms is beyond the scope of this study, some possible sources of internal wave energy on the Southeast Florida shelf are: (1) the adjustment of density interfaces corresponding to instabilities in the Florida Current or to the Ekman and arrested boundary layer regimes on the stratified western slope of the Straits of Florida [*MacCready and Rhines*, 1993; *Seim et al.*, 1999], (2) the development of instabilities on the steepening face of the internal tide [*Baines*, 1986;

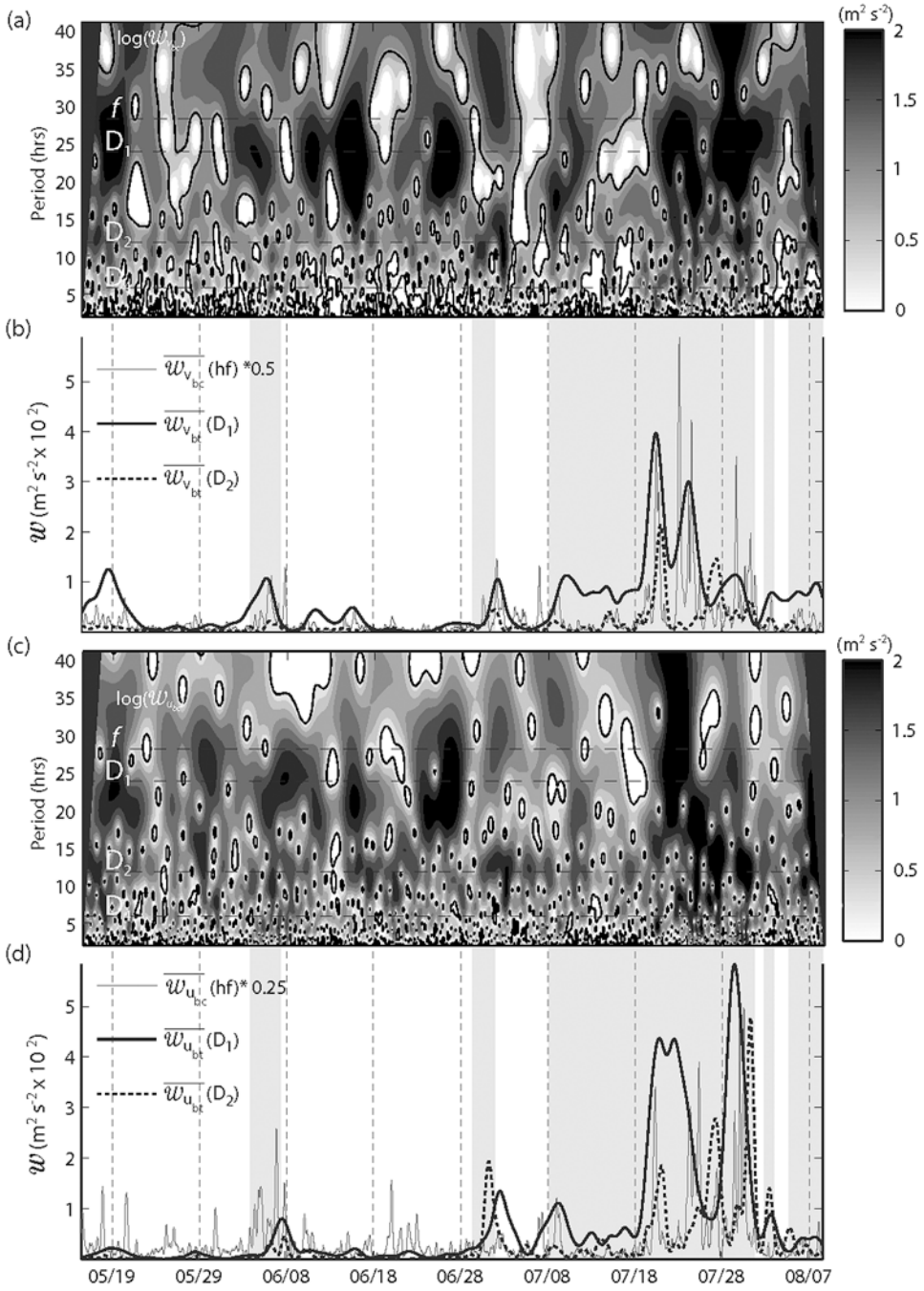

Figure 9. Baroclinic current wavelet spectra from Mooring D, summer 2003: (a) logarithm of the wavelet power spectrum for CEOF amplitude of v_{bc}, $\mathcal{W}_{v_{bc}} = |\mathcal{W}_{v_{bc}}(s)|^2$ (b) high frequency band-averaged $\mathcal{W}_{v_{bc}}$, D_1 and D_2 band-averaged $\mathcal{W}_{v_{bt}}$, (c) logarithm of the wavelet power spectrum for CEOF amplitude of u_{bc}, $\mathcal{W}_{u_{bc}} = |\mathcal{W}_{u_{bc}}(s)|^2$ (d) high frequency band-averaged $\mathcal{W}_{u_{bc}}$, D_1 and D_2 band-averaged $\mathcal{W}_{u_{bt}}$. In panels (a) and (c) the thick black lines are 95% confidence level and dashed horizontal lines mark the major tidal (D_1 is diurnal and D_2 is semidiurnal) and inertial (f) periods. Darkly shaded regions on either side of the wavelet spectra indicate the ''cone of influence'' where edge effects become important. In panels (b) and (d) the high frequency band-averaged W are multiplied by a factors of 0.5 and 0.25, respectively for visualization purposes.

Colosi et al., 2001], and (3) the critical reflection of internal waves on the slope, and propagation of this energy upslope as NLIWs [*Ivey and Nokes*, 1989].

[42] The geometry of the slope offshore of the study site (see Figure 2) is conducive to the critical reflection of semidiurnal band internal waves. Energy from critically reflected waves can be transferred into bottom-intensified

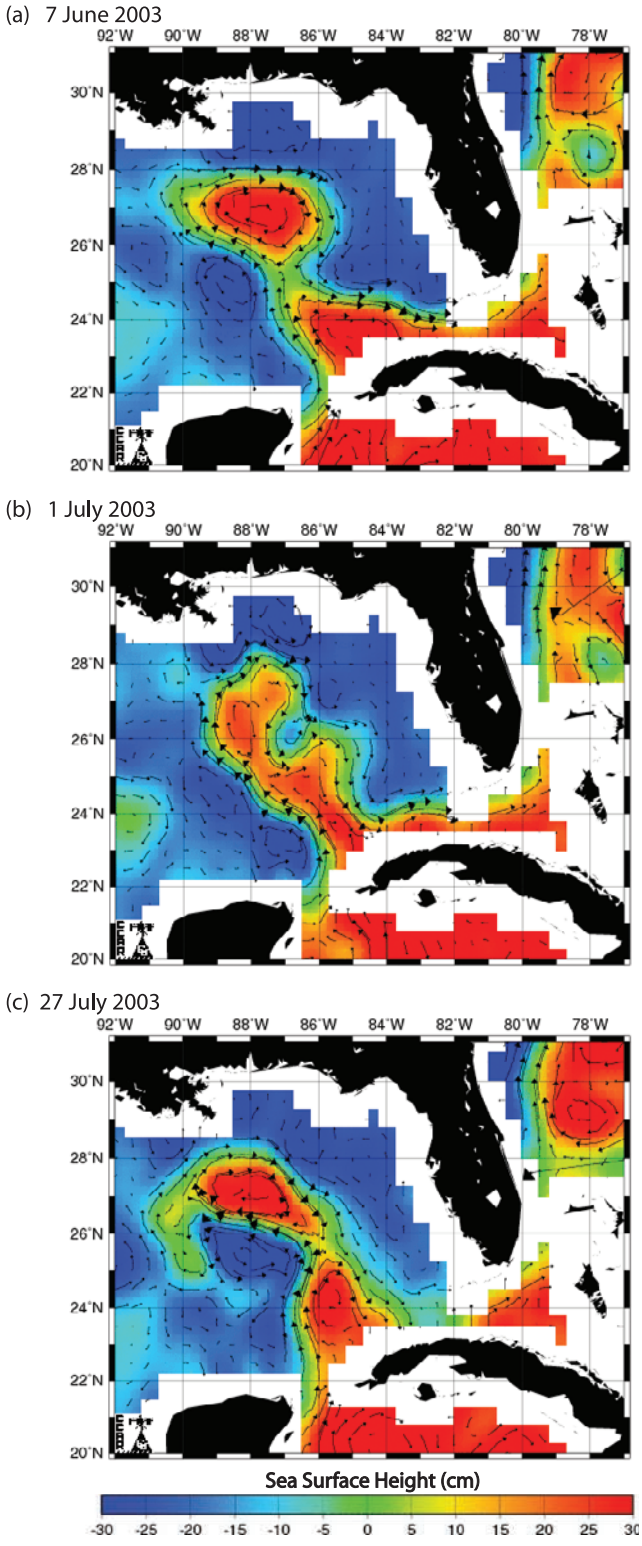

Figure 10. Sea surface height contours derived from satellite altimetry images of the Gulf of Mexico and Straits of Florida with superimposed geostrophic velocity vectors during the 2003 Conch Reef experiment. Images were obtained from the Colorado Center for Astrodynamics Research, University of Colorado, Boulder.

currents parallel to the slope [*Cacchione et al.*, 2002]. Observations of intermittent, near-bed incursions of cool water on the outer shelf and near-bed maxima in both semidiurnal and high-frequency band $\sigma^2_{u_{bc}}$ at Mooring D (Figures 7a and 7b) are consistent with the transfer of tidal period baroclinic energy into high-frequency, nonlinear internal waves and bores on the slope at or just offshore of Mooring D. Additional evidence for this theory is the shoreward decay in the size of the semidiurnal baroclinic ellipses (Figure 8) coupled with a shoreward increase in the percentage of $\sigma_{u_{bc}}{}^2$ accounted for by high-frequency processes: 74%, 64%, and 71% respectively for Moorings A, B, and C, as opposed to 39% for Mooring D, indicating a blue shift of the internal wave spectrum across the shelf. Near-bed temperature variability on Conch Reef observed during this study and *Leichter and Miller* [1999] is consistent with the baroclinic current observations.

[43] Near-bed semidiurnal band baroclinic currents are not however significantly correlated with near-bed high-frequency band currents at Mooring D, suggesting that the internal tide and high-frequency waves are not generally coincident at this location. This result could be explained as two modes of internal wave activity at Mooring D, where near-bed baroclinic currents of semidiurnal frequency correspond to periods when the internal tide runs up on the slope unbroken, and periods with predominantly high-frequency near-bed currents occur when the internal tide breaks downslope and the tidal energy is transferred into higher-frequency waves or bores which propagate shoreward. Another explanation for this finding is that the high-frequency internal waves are not associated with internal tide, but are instead generated by another mechanism offshore and dissipate on the shallow slope.

[44] The Florida Current can affect the internal wave field on the narrow Southeast Florida shelf directly by generating internal waves off of fronts or eddies, or indirectly by modifying stratification and shear conditions at the shelf-break. Evidence for the link between the high-frequency internal wave energy on Conch Reef and instabilities from the FC can be seen in the visual correlation between peaks in the high-frequency, baroclinic $\overline{\mathcal{W}}$ and the shaded patches indicating the passage of an eddy through the study site (Figures 9b and 9d). This result is supported by observations from a 2001 study in the Upper Florida Keys by *Sponaugle et al.* [2005] which found the passage of eddies to be accompanied by a period of increased tidal bore activity. Equivalent correlation values between the high-frequency baroclinic currents and both the diurnal and semidiurnal barotropic currents suggest that the dynamics of the FC play as large a role in the determination of the high-frequency internal wave field on the outer Southeast Florida shelf as the tide.

[45] The dynamics of cross-shelf circulation have important consequences for organisms living on the shelf. Previous observations have demonstrated that both mesoscale frontal eddies [*Sponaugle et al.*, 2005] and internal waves [*Leichter et al.*, 2003] can contribute to the exchange of heat, nutrients, and larvae across the Southeast Florida shelf. Observations from this study provide further evidence that internal waves play an important role in cross-shelf exchange, particularly internal waves in the high-frequency band (<5 hours). During periods of elevated internal wave

activity on Conch Reef, we found that up to 90% of the variance in the across-shelf velocity was accounted for by baroclinic modes, and of this, high-frequency band processes were dominant (Figure 7). This suggests that cross-shelf exchange may be as episodic as the high-frequency internal wave field and that estimating cross-shelf exchange using surface current observations alone [e.g., *Haus et al.*, 2004] could be a significant underestimate.

7. Conclusions

[46] Previous work on the Southeast Florida shelf has led to speculation that the internal wave field may be affected by instabilities in the Florida Current in addition to tidal forces [*Leichter et al.*, 2003; *Soloviev et al.*, 2003]. In this study, we provide evidence for this link through the nonstationary spectral analysis of the complex and unsteady currents on the outer shelf. Wavelet analyses of the barotropic current (Figure 4) coupled with concurrent altimetry images of the Straits of Florida (Figure 10) reveal the strong influence of Florida Current fluctuations on outer shelf flows. A shift in flow regime on the outer shelf correlates with a change in the location of the FC axis offshore and the passage of multiple frontal eddies. The propagation of a frontal eddy through the study site is associated with a peak in diurnal band spectral power in the barotropic currents (Figure 4). Tidal forcing (diurnal and semidiurnal) accounted for 23–32% of the variance in barotropic currents and local winds were found to be an insignificant factor in flows on the outer shelf, which is in agreement with previous studies in the Upper Florida Keys [*Lee and Mayer*, 1977; *Lee*, 1986].

[47] High-frequency internal waves dominate the internal wave field on the outer Southeast Florida shelf (Figure 7). The geometry of the slope offshore of the study site (Figure 2), observations of near-bed maxima in semidiurnal and high-frequency variance (Figure 7), as well as the shoreward decrease in the size of semidiurnal baroclinic ellipses (Figure 8) support the idea that the high-frequency internal waves on the shelf are generated by the critical reflection of the semidiurnal internal tide on the continental slope. However the episodic nature of the observed high-frequency internal wave field suggests that the internal wave climate is modified by something in addition to periodic tidal forcing. We found high-frequency band baroclinic $\overline{\mathcal{U}}$ to be significantly correlated (r = 0.40) with both diurnal and semidiurnal band barotropic $\overline{\mathcal{U}}$, suggesting that the FC play as large a role in the determination of the internal wave field as the tide. Instabilities in the FC cause significant aperiodic variation in offshore shear and stratification. This variation modifies the conditions under which the tide interacts with the topography to generate waves and the environment through which those waves propagate and thus can affect the internal wave field on the outer shelf. These observations and analyses show that it is necessary to include the forcing from the FC meanders and instabilities in order to predict accurately the episodic nature of the internal wave field on the Southeast Florida shelf.

[48] **Acknowledgments.** Field support and ship time for this study were generously provided by the National Undersea Research Center in Key Largo, Florida. We also thank the captain and crew of the *R/V Walton-Smith* and staff of the Marine Operations Department of the Rosenstiel School of Marine and Atmospheric Sciences for logistic support. We thank Greg Shellenbarger, Mike Murray, and Amatzia Genin for diving assistance and Adina Paytan and Derek Fong for providing field support. We also acknowledge valuable discussions with Greg Ivey, Eric Kunze, and Leif Thomas and the helpful advice of two anonymous reviewers. Funding was provided by grants from the National Oceanic and Atmospheric Administration's National Undersea Research Program to JJL and SGM as well as a Career Development Award from the E.W. Scripps Associates to JJL, and National Science Foundation grants OCE-0452800 and OCE-0622967 to SGM and JLH. Kristen Davis was supported by a National Defense Science and Engineering Graduate Fellowship.

References

Baines, P. G. (1986), Internal tides, internal waves, and near-inertial motions, in *Baroclinic Processes on Continental Shelves*, edited by C. N. K. Mooers, pp. 19–31, AGU, Washington, D. C.

Boudra, D. B., R. Bleck, and F. Schott (1988), A numerical model of instabilities in the Florida Current, *J. Mar. Res.*, *46*, 715–751.

Brooks, I. H. (1979), Fluctuations in the transport of the Florida Current at periods between tidal and two weeks, *J. Phys. Oceanogr.*, *9*, 1048–1053.

Cacchione, D. A., L. F. Pratson, and A. S. Ogston (2002), The shaping of continental slopes by internal tides, *Science*, *296*, 724–727.

Colosi, J. A., R. C. Beardsley, J. F. Lynch, G. Gawarkiewicz, C.-S. Chiu, and A. Scotti (2001), Observations of nonlinear internal waves on the outer New England continental shelf during the summer Shelfbreak Primer study, *J. Geophys. Res.*, *106*(C5), 9587–9601.

Efron, B., and T. J. Tibshirani (1993), *An Introduction to the Bootstrap*, 436 pp., Chapman and Hall, London.

Farge, M. (1992), Wavelet transforms and their applications to turbulence, *Annu. Rev. Fluid Mech.*, *24*, 395–457.

Gill, A. E. (1982), *Atmosphere-Ocean Dynamics*, 662 pp., Academic Press, San Diego.

Ginsburg, R. N., E. Gischler, and W. E. Kiene (2001), Partial mortality of massive reef-building corals: An index of patch reef condition, Florida Reef Tract., *Bull. Mar. Sci.*, *69*(3), 1149–1173.

Hales, B., J. N. Moum, P. Covert, and A. Perlin (2005), Irreversible nitrate fluxes due to turbulent mixing in a coastal upwelling system, *J. Geophys. Res.*, *110*, C10S11, doi:10.1029/2004JC002685.

Haus, B. K., J. D. Wang, J. Rivera, J. Martinez-Pedraja, and N. Smith (2000), Remote radar measurement of shelf currents off Key Largo, Florida, U.S.A., *Estuar. Coast. Shelf Sci.*, *51*, 553–569.

Haus, B. K., J. D. Wang, J. Martinez-Padraja, and N. Smith (2004), Southeast Florida Shelf circulation and volume exchange, observations of km-scale variability, *Estuar. Coast. Shelf Sci.*, *59*, 277–294.

Henyey, F. S., and A. Hoering (1997), Energetics of borelike internal waves, *J. Geophys. Res.*, *102*(C2), 3323–3330.

Hosegood, P., J. Bonnin, and H. V. Haren (2004), Solibore-induced sediment resuspension in the Faeroe-Shetland Channel, *Geophys. Res. Lett.*, *31*, L09301, doi: 10.1029/2004GL019544.

Inall, M. E., T. P. Rippeth, and T. J. Sherwin (2000), Impact of nonlinear waves on the dissipation of internal tidal energy at a shelf break, *J. Geophys. Res.*, *105*(C4), 8687–8705.

Ivey, G. N., and R. I. Nokes (1989), Vertical mixing due to the breaking of critical internal waves on sloping boundaries, *J. Fluid Mech.*, *418*, 59–76.

Ivey, G. N., K. B. Winters, and I. P. D. DeSilva (2000), Turbulent mixing in a sloping benthic boundary layer energized by internal waves, *J. Fluid Mech.*, *418*, 59–76.

Jaap, W. C. (1984), *The Ecology of the South Florida Coral Reefs: A Community Profile*, pp. 138, Florida Department of Natural Resources, Marine Research Laboratory, St. Petersburg.

Jay, D. A., and T. Kukulka (2003), Revising the paradigm of tidal analysis—the uses of non-stationary data, *Ocean Dyn.*, *53*, 110–125.

Kielmann, J., and W. Duing (1974), Tidal and sub-inertial fluctuations in the Florida current, *J. Phys. Oceanogr.*, *4*, 227–236.

Klymak, J. M., and J. N. Moum (2003), Internal solitary waves of elevation advancing on a shoaling shelf, *Geophys. Res. Lett.*, *30*(20), 2045, doi:10.1029/2003GL017706.

Kunze, E. (1985), Near-inertial waves propagation in geostrophic shear, *J. Phys. Oceanogr.*, *15*, 544–565.

Lamb, K. G. (2003), Shoaling solitary internal waves: On a criterion for the formation of waves with trapped cores, *J. Fluid Mech.*, *478*, 81–100.

Leben, R. R., G. H. Born, and B. R. Engebreth (2002), Operational altimeter processing for mesoscale monitoring, *Mar. Geod.*, *25*, 3–18.

Ledwell, J. R., T. F. Duda, M. A. Sundermeyer, and H. E. Stein (2004), Mixing in a coastal environment: 1. A view from dye dispersion, *J. Geophys. Res.*, *109*, C10013, doi:10.1029/2003JC002194.

Lee, T. N. (1975), Florida current spin-off eddies, *Deep Sea Res.*, *22*, 753–765.

Lee, T. N., and D. A. Mayer (1977), Low-frequency variability and spin-off

eddies along the shelf off Southeast Florida, *J. Mar. Res.*, *35*(1), 193–220.
Lee, T. N., L. P. Atkinson, and R. Legeckis (1981), Observations of a Gulf Stream frontal eddy on the Georgia continental shelf, April 1977, *Deep Sea Res.*, *28A*(4), 347–378.
Lee, T. N. (1986), Coastal circulation in the Key Largo Coral Reef Marine Sanctuary, in *Physics of Shallow Estuaries and Bays*, edited by J. V. D. Kreeke, pp. 178–198, Springer, Berlin.
Lee, T. N., and E. Williams (1988), Wind-forced transport fluctuations of the Florida Current, *J. Phys. Oceanogr.*, *18*, 937–946.
Lee, T. N., K. Leaman, E. Williams, T. Berger, and L. Atkinson (1995), Florida current meanders and gyre formation in the southern Straits of Florida, *J. Geophys. Res.*, *100*(C5), 8607–8620.
Leichter, J. J., S. R. Wing, S. L. Miller, and M. W. Denny (1996), Pulsed delivery of subthermocline water to Conch Reef (Florida Keys) by internal tidal bores, *Limnol. Oceanogr.*, *41*(7), 1490–1501.
Leichter, J. J., G. Shellenbarger, S. J. Genovese, and S. R. Wing (1998), Breaking internal waves on a Florida (USA) coral reef: a plankton pump at work?, *Mar. Ecol. Prog. Ser.*, *166*, 83–97.
Leichter, J. J., and S. L. Miller (1999), Predicting high-frequency upwelling: Spatial and temporal patterns of temperature anomalies on a Florida coral reef, *Cont. Shelf Res.*, *19*, 911–928.
Leichter, J. J., H. L. Stewart, and S. L. Miller (2003), Episodic nutrient transport to Florida coral reefs, *Limnol. Oceanogr.*, *48*(4), 1394–1407.
Leichter, J. J., G. B. Deane, and M. D. Stokes (2005), Spatial and temporal variability of internal wave forcing on a coral reef, *J. Phys. Oceanogr.*, *35*, 1945–1962.
Leichter, J. J., A. Paytan, S. Wankel, K. Hanson, S. Miller, and M. A. Altabet (2007), Nitrogen and oxygen isotopic signatures of subsurface nitrate seaward of the Florida Keys reef tract, *Limnol. Oceanogr.*, *52*(3), 1258–1267.
Leichter, J. J., M. D. Stokes, and S. J. Genovese (2008), Deep water macroalgae seaward of the Florida Keys, USA, *Mar. Ecol. Prog. Ser.*, *356*, 123–138.
Liu, A. K., Y. S. Chang, M.-K. Hsu, and N. K. Liang (1998), Evolution of nonlinear internal waves in the East and South China Seas, *J. Geophys. Res.*, *103*(C4), 7995–8008.
Liu, P. C., and G. S. Miller (1996), Wavelet transforms and ocean current data analysis, *J. Atmos. Oceanic Technol.*, *13*, 1090–1099.
Lu, Y., and R. G. Lueck (1999), Using a broadband ADCP in a tidal channel. Part 1: Mean flow and shear, *J. Atmos. Oceanic Technol.*, *16*, 1556–1567.
MacCready, P., and P. B. Rhines (1993), Slippery bottom boundary layers on a slope, *J. Phys. Oceanogr.*, *23*, 5–22.
McKee, W. D. (1973), Internal-inertial waves in a fluid of variable depth, *Math. Proc. Cambridge*, *73*, 205–213.
Munk, W., and C. Wunsch (1998), Abyssal recipes II: Energetics of tidal and wind mixing, *Deep Sea Res., Part 1*, *45*, 1977–2010.
Niiler, P. P. (1968), On the internal tidal motions in the Florida Straits, *Deep Sea Res.*, *15*, 113–123.
Parr, A. E. (1937), Report on hydrographic observations at a series of anchor stations across the Straits of Florida, *Bull. Bingham Oceanogr. Coll.*, *6*(3), 1–63.
Phillips, O. M. (1977), *The Dynamics of the Upper Ocean*, Cambridge Univ. Press, Cambridge.
Pineda, J. (1991), Predictable upwelling and the shoreward transport of planktonic larvae by internal tidal bores, *Science*, *253*, 548–551.
Preisendorfer, R. W. (1988), *Principal Component Analysis in Meteorology and Oceanography*, 425 pp., Elsevier, Amsterdam.
Pringle, J. M., and K. H. Brink (1999), High-frequency internal waves on a sloping shelf, *J. Geophys. Res.*, *104*(C3), 5283–5299.
Qiu, L. J., and M. H. Er (1995), Wavelet spectrogram of noisy signals, *Int. J. Electron.*, *79*, 665–677.
Riegl, B., and W. E. Piller (2003), Possible refugia for reefs in times of environmental stress, *Int. J. Earth Sci. (Geol. Rundsch.)*, *92*, 520–531.
Sanford, L. P., and W. D. Grant (1987), Dissipation of internal wave energy in the bottom boundary layer on the continental shelf, *J. Geophys. Res.*, *92*(C2), 1828–1844.
Schmitz, W. J., and W. S. Richardson (1968), On the transport of the Florida current, *Deep Sea Res., Part X*, *15*, 679–693.
Schott, F., and W. Duing (1976), Continental shelf waves in the Florida Straits, *J. Phys. Oceanogr.*, *6*, 451–460.
Schott, F. A., T. N. Lee, and R. Zantopp (1988), Variability of structure and transport of the Florida Current in the period range of days to seasonal, *J. Phys. Oceanogr.*, *18*, 1209–1230.
Scotti, A., and J. Pineda (2004), Observation of very large and steep internal waves of elevation near the Massachusetts coast, *Geophys. Res. Lett.*, *31*, L22307, 10.1029/2004GL021052.
Scotti, A., B. Butman, R. C. Beardsley, P. S. Alexander, and S. Anderson (2005), A modified beam-to-earth transformation to measure short-wavelength internal waves with an acoustic Doppler current profiler, *J. Atmos. Oceanic Technol.*, *22*, 583–591.
Seim, H. E., D. P. Winkel, G. Gawarkiewicz, and M. C. Gregg (1999), A benthic front in the Florida Straits and its relationship to the structure of the Florida Current, *J. Phys. Oceanogr.*, *29*, 3125–3132.
Sharples, J., C. M. Moore, and E. R. Abraham (2001), Internal tide dissipation, mixing, and vertical nitrate flux at the shelf edge of NE New Zealand, *J. Geophys. Res.*, *106*(C7), 14,069–14,081.
Shay, L. K., T. N. Lee, E. J. Williams, H. C. Graber, and C. C. H. Rooth (1998), Effects of low-frequency current variability on near-inertial submesoscale vortices, *J. Geophys. Res.*, *103*(C9), 18,691–18,714.
Soloviev, A. V., M. E. Luther, and R. H. Weisburg (2003), Energetic baroclinic super-tidal oscillations on the southeast Florida shelf, *Geophys. Res. Lett.*, *30*(9), 1463, doi:10.1029/2002GL016603.
Sponaugle, S., T. Lee, V. Kourafalou, and D. Pinkard (2005), Florida Current frontal eddies and the settlement of coral reef fishes, *Limnol. Oceanogr.*, *50*(4), 1033–1048.
Stacey, M. T., J. R. Burau, and S. G. Monismith (2001), Creation of residual flows in a partially stratified estuary, *J. Geophys. Res.*, *106*(C8), 17,013–17,037.
Stommel, H. M. (1958), *The Gulf Stream: A Physical and Dynamical Description*, Univ. of California Press, Berkeley.
Torrence, C., and G. P. Compo (1998), A practical guide to wavelet analysis, *Bull. Am. Meteorol. Soc.*, *79*(1), 61–78.
Wunsch, C. (1969), Progressive internal waves on slopes, *J. Fluid Mech.*, *35*, 131–144.

K. A. Davis, J. L. Hench, and S. G. Monismith, Environmental Fluid Mechanics Laboratory, Stanford University, Yang and Yamasaki Environment and Energy Building, 473 Via Ortega, Stanford, CA 94305-4020, USA. (kristen.davis@stanford.edu)

J. J. Leichter, Scripps Institution of Oceanography, University of California, San Diego, 9500 Gilman Drive, La Jolla, CA 92093-0227, USA.